Global and gene specific DNA methylation in breast cancer cells was not affected during epithelial-to-mesenchymal transition *in vitro*

B. SMOLKOVA[1,*], S. MIKLIKOVA[1], V. HORVATHOVA KAJABOVA[1], A. BABELOVA[1], N. EL YAMANI[2], M. ZDURIENCIKOVA[1], I. FRIDRICHOVA[1], I. ZMETAKOVA[1], T. KRIVULCIK[1], L. KALINKOVA[1], M. MATUSKOVA[1], L. KUCEROVA[1], M. DUSINSKA[2]

[1]Cancer Research Institute, Biomedical Research Center, Slovak Academy of Sciences, Bratislava, Slovakia; [2]Norwegian Institute for Air Research, Kjeller, Norway

*Correspondence: bozena.smolkova@savba.sk

Epithelial-to-mesenchymal transition (EMT) significantly affects the risk of metastasising in breast cancer. Plasticity and reversibility of EMT suggest that epigenetic mechanisms could be the key drivers of these processes, but little is known about the dynamics of EMT-related epigenetic alterations. We hypothesised that EMT, mediated by autocrine and paracrine signals, will be accompanied by changes in DNA methylation profiles. Therefore, conditioned medium from adipose tissue-derived mesenchymal stromal cells was used for induction of EMT in human breast cancer SK-BR-3 cell line. EMT-related morphological alterations and changes in gene expression of EMT-associated markers were assessed. To reverse EMT, 20 nm size gold nanoparticles (AuNPs) synthesized by the citrate reduction method were applied. Finally, DNA methylation of LINE-1 sequences and promoter methylation of *TIMP3*, *ADAM23* and *BRMS1* genes were quantitatively evaluated by pyrosequencing. Despite the presence of EMT-associated morphological and gene expression changes in tumour cells, EMT induced by adipose tissue-derived mesenchymal stromal cells had almost no effect on LINE-1 and gene-specific DNA methylation patterns of *TIMP3*, *ADAM23* and *BRMS1* genes. Although treatment for 24, 48 or 72 hours with 20 nm AuNPs at a concentration of 3 µg/ml slightly decreased gene expression of EMT-associated markers in SK-BR-3 cells, it did not alter global or gene-specific DNA methylation. Our results suggest that changes in DNA methylation are not detectable *in vitro* in early phases of EMT. Previously published positive findings could represent rather the sustained presence of potent EMT-inducing signals or the synergistic effect of various epigenetic mechanisms. Treatment with AuNPs slightly attenuated EMT, and their therapeutic potential needs to be further investigated.

Key words: DNA methylation, mesenchymal stromal cells, epithelial-to-mesenchymal transition, gold nanoparticles, breast cancer

In a majority of cancers, including breast cancer (BC), mortality is caused by metastases rather than primary tumours. Genesis of metastases is believed to be preceded by dissemination of tumour cells into the blood circulation or lymphatic channels, which is determined by their morphological and functional dedifferentiation from the epithelial to mesenchymal phenotype. This complex process, known as epithelial-to-mesenchymal transition (EMT), leads to an increased motility and loss of cell adhesion. EMT is an extreme example of cell plasticity that was reported as a key regulator of metastatic spread. Active recruitment of cells, including mesenchymal stromal cells (MSCs) into the tumour microenvironment and production of a unique set of growth factors and chemokines, may play an important role in malignant progression [1, 2]. Adipose tissue-derived stromal cells (AT-MSCs) – a mesenchymal cell population, able to differentiate toward osteogenic, adipogenic, myogenic, and chondrogenic lineages [3] – are present in the adipose tissue, the most abundant stromal constituent of breast. As they can integrate into tumour-associated stroma and exhibit multiple regulatory functions, they can contribute to mammary carcinogenesis [4-6]. Similarly to bone marrow-derived MSCs, they were demonstrated to promote EMT [2, 7]. Recent investigation of the mechanisms controlling EMT revealed a significant epigenetic regulatory impact (reviewed in [8]). Cells in their epigenetically plastic state could be programmed by the microenvironment, to acquire epigenetic changes associated with tumourigenesis

and induction of EMT. Widespread epigenetic reprogramming occurs during stem cell differentiation and malignant transformation [9], but EMT-related epigenetic alterations are poorly understood.

Gold nanoparticles (AuNPs) have attracted wide attention in various biomedical applications due to their chemical stability, electrondense core and ease of conjugation to drugs and biomolecules [10]. Their antiangiogenic and antimetastatic potential was demonstrated recently *in vitro* by their ability to inhibit the function of heparin-binding growth factor proteins [11, 12]. Since these proteins are critically important for EMT and angiogenesis, AuNPs may provide novel therapeutic possibilities in preventing tumour growth and metastasising [5]. Although AuNPs are generally thought to be inert and non-toxic, their possible epigenetic toxicity has been investigated rarely [13, 14]. In the present study we analyzed the therapeutic potential of AuNPs mediated by their proposed ability to reverse EMT.

Further understanding of the interactions between MSCs and tumour cells in terms of the EMT process is important to determine their role in BC progression as well as to assess their safety for utilization in cell therapies and regenerative medicine. To investigate possible EMT-related epigenetic changes, we analyzed global DNA methylation levels in long interspersed nuclear element-1 (LINE-1) sequences and three metastasis-associated genes, namely a disintegrin and metalloprotease domain 23 (*ADAM23*), tissue inhibitor of metalloproteinases 3 (*TIMP3*) and breast cancer metastasis suppressor 1 (*BRMS1*). Selection of genes was based on their previously published association with EMT [15] and haematogenous metastasising [16].

Material and methods

Cell cultures. The human breast cancer cell line SK-BR-3 (ATCC® Number HTB-30™) was used for the study. Tumour cells were maintained in high-glucose (4.5 g/l) DMEM (PAA Laboratories GmbH, Pasching, Austria) containing 10% FBS (Biochrom AG, Berlin, Germany), 10.000 IU/ml penicillin (Biotika, Slovenska Lupca, SK), 5 μg/ml streptomycin, 2 mM glutamine and 2.5 μg/ml amphotericin (PAA Laboratories GmbH, Pasching, Austria).

MSCs derived from adipose tissue were supplied by the Department of Plastic, Aesthetic and Reconstructive Surgery, University Hospital, Bratislava. Following a defined clinical protocol, liposuction aspirates were obtained from healthy donors who provided written informed consent. AT-MSCs isolated and characterized as described previously [17] were used to induce EMT in SK-BR-3 cells by cell-free AT-MSC-conditioned medium (MSC-CM). MSC-CM was collected from 80–90% confluent AT-MSC cultures after 24 hours of cultivation with fresh tumour cell culture medium (DMEM) and filtered through 0.45 μm filters. SK-BR-3 tumour cells were cultured with MSC-CM, without presence of AT-MSC cells, for 9 days with medium replenishment every 3 days.

Changes in cell biology were evaluated by kinetic live cell imaging (IncuCyte ZOOM™ Kinetic Imaging system (Essen BioScience, UK)) and fluorescent microscopy (Axiovert 200, Zeiss, Germany). Phase-contrast images were taken after 6 days in DMEM or MSC-CM cultivation every two hours for next 72 hours. Total RNA and DNA were isolated from high-glucose DMEM and MSC-CM-cultivated cells.

Nanoparticles. AuNPs of size 20 nm synthesized by the citrate reduction method, purchased from Ted Pella Inc., were used for the experiments without any further modification. Prior to *in vitro* experiments particle size distribution and concentration were determined using NanoSight NS500 instrument (Malvern Instruments Ltd., UK) equipped with a 405nm laser and sCMOS Trigger camera. This method is based on visualising and tracking the light scattered from each particle in solution undergoing Brownian motion. Data were analyzed by Nanoparticle Tracking Analysis (NTA) 2.3 software provided by the manufacturer. Samples were measured four times for a period of 60 seconds. All measurements were performed at room temperature.

Proliferation assay – relative cell growth activity (RGA). Four concentrations of AuNPs, ranging from 0.8 – 28 μg/ml were tested with the RGA assay, to assess non-cytotoxic concentrations for further experiments. SK-BR-3 cells were seeded on 96-well plates (2.8×10^4 cells per well) and incubated at 37°C. After 24 hours the cells were exposed to 20 nm AuNPs for 2, 24 and 48 hours. At the end of the exposure period, 10 μl of trypsinized cells (resuspended in 1 ml of medium) were mixed with 10 μl 0.4% trypan blue (Invitrogen, Carlsbad, CA). The percentages of living and dead cells were measured using a Countess™ Automated Cell Counter (Invitrogen, Carlsbad, CA). Measurements were performed immediately upon staining (for all three exposure times). Results express means of two independent experiments.

RGA was calculated according to the following formula:

$$RGA(\%) = \frac{\text{number of living cells at day n/ number of seeded cells at day 0) in exposed cultures}}{\text{number of living cells at day n / number of seeded cells at day 0) in unexposed cultures}} \times 100\%$$

Gene expression analyses. Total RNA was isolated by NucleoSpin RNA kit (Machery Nagel, Düren, Germany) and reverse transcribed with a RevertAid H minus First Strand cDNA synthesis kit (Fermentas, Amherst, NY). Semiquantitative real-time PCR was performed with Brilliant III Ultra-Fast SYBR Green QPCR Master Mix (Agilent Technologies, Palo Alto, CA), 0.2 μM primers and 75 ng of the template cDNA on Bio-Rad CFX96™ with pre-set amplification profile and analyzed by Bio-Rad CFX Manager software version 1.6. Primer sequences for snail family zinc finger 1 (*SNAI1*), snail family zinc finger 2 (*SNAI2*), twist family BHLH transcription factor 1 (*TWIST1*), fibroblast-activation protein (*FAP*) and alpha-smooth muscle actin (*α-SMA*) were identical

as published previously [7]. Annealing temperatures were adjusted using gradient PCR to attain optimal amplification efficiency (90–105%) for all analyzed targets. Optimal annealing temperatures were set at 55°C for *SNAI1*, *SNAI2*, *TWIST1*, *FAP* and 57°C for *α-SMA* genes. Relative expressions of target genes normalized to *HPRT* were calculated by the ΔΔCt method. TaqMan Hs01023894_m1 (*CDH1*) and Hs99999905_m1 (*GAPDH*) gene expression assays were used to analyse *CDH1* gene expression. Analysis of gene expression data was performed using the relative expression software tool REST© [18].

Immunohistochemistry. Cells were washed with PBS and fixed with 4% PFA for 20 minutes. After incubation with anti-F-actin rhodamine-labeled antibody (Molecular Probes), nuclei were counterstained with DAPI. Staining patterns were analyzed with a Zeiss fluorescent microscope and automated imaging Metafer (MetaSystems GmbH, Germany).

DNA extraction and sodium bisulfite modification. DNA from cell cultures (1-2 x 10^6 cultured cells) was obtained using a FlexiGene DNA kit (Qiagen, Hilden, Germany) according to the manufacturer's instructions. Sodium bisulfite treatment of extracted DNA (2 μg) was performed using an established protocol of the EpiTect Bisulfite Kit (Qiagen, Hilden, Germany). This process replaces unmethylated cytosine residues with uracil while methylated cytosines remain unaltered, giving rise to two different sequences that can be distinguished in methylation analysis.

Pyrosequencing. Quantification of the methylation level of the LINE-1 retrotransposable elements and gene-specific promoter methylation of three selected genes *TIMP3*, *ADAM23* and *BRMS1* was performed by pyrosequencing. Global DNA methylation was analyzed with the PyroMark Q24 CpG LINE-1 kit (Qiagen, Hilden, Germany). This methylation detection assay uses real time, sequence-based Pyrosequencing® technology to quantify the methylation levels of three CpG sites in positions 331 to 318 of the LINE-1 sequence (GenBank accession number X58075). The first step was the amplification of a 146 bp fragment using bisulfite-treated DNA by PCR reactions, as described in the PyroMark PCR Kit (Qiagen, Hilden, Germany) protocol. Forward and reverse PCR primers and sequencing primer for LINE-1 analyses were provided by the PyroMark Q24 CpG LINE-1 kit (Qiagen, Hilden, Germany). Gene-specific DNA methylation was detected as published previously [19]. Pyrosequencing runs were carried out using a PyroMark Q24 system and the PyroMark Gold Q24 Reagens (Qiagen, Hilden, Germany) according to the manufacturer's protocol. The results of the analyses were evaluated using the PyroMark Q24 2.0.6. software (Qiagen, Hilden, Germany). Methylation data are presented as the percentage of average methylation in three to nine CpG sites depending on the analyzed gene.
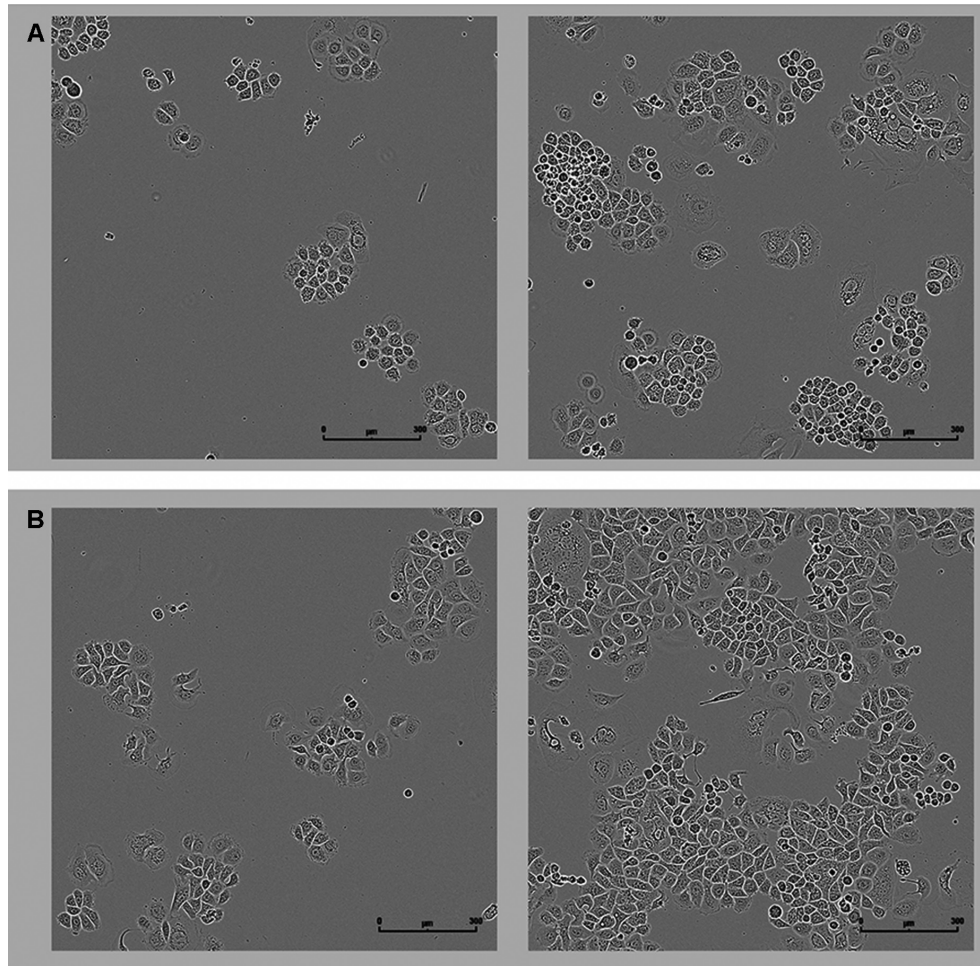
Statistical analysis. The independent samples t-test for normally distributed data and the Mann-Whitney U-test for non-normally distributed data were used to test for significant differences between groups. Differences between more

than two groups were tested by one-way analysis of variance (ANOVA) and by Bonferroni´s or Tamhane´s test depending on assumed variances. SPSS 15.0 software was used for statistical analysis. Differences with P <0.05 were considered to be statistically significant.

Results and discussion

AT-MSCs released factors induce EMT in BC cells. MSCs have been reported to be actively recruited to the primary tumour stroma. This tumour-homing ability makes them an attractive treatment tool for delivering anti-cancer agents to tumour environments [20]. However, the safety of such approaches remains unresolved [21]. Published reports, showing interaction between MSCs and cancer cells with subsequent promotion of their metastatic potential, call for further elucidation of these processes [6]. Despite the minor differences between studied MSC populations, similarities between bone marrow and adipose tissue-derived MSCs [22] and breast and abdominal-derived adipose tissues MSCs [23] have been demonstrated. Based on previously published results [7], we used a similar approach for EMT induction using MSC-CM in the SK-BR-3 cell line. EMT was successfully induced by 6-9 days cultivation of tumour cells in MSC-CM. The MSC-CM-cultivated SK-BR-3 cells presented altered morphology compared to DMEM-cultivated cells after 6 days of cultivation (Figure 1). Their shape changed from the epithelial-like cobblestone to the spindle-like fibroblastoid features. Newly acquired mesenchymal-like phenotype was typical with scattered colony appearance and increased confluence. These results, supporting the presence of EMT, were confirmed by immunohistochemical staining of F-actin (Figures 2A and 2B) and analyses of gene expression (Figure 3). After 6 days of cultivation we found up-regulation of EMT-associated markers, but only *FAP* expression was increased significantly in MSC-CM cultured cells, while all analysed EMT markers were significantly up-regulated after 9 days of cultivation (Figure 3). Similar results were reported previously by Kucerova et al., who showed altered tumour cell morphology, induced EMT, increased mammosphere formation, cell confluence and migration by cultivation of SK-BR-3 cells with AT-MSCs or MSC-CM, respectively [7]. The authors reported similar morphological changes but relatively stronger up-regulation of gene expression of EMT-associated markers, ranging from 2 to nearly 1000 times. These results were gained after 6 days of MSC-CM cultivation with everyday medium replenishment, in contrast to our method where medium was replenished every 3 days. Heterogeneity of the MSC samples used to derive the CM, could also explain these findings. Similarly to our results Iser et al. showed that conditioned medium from adipose-derived stem cells changed cell morphology of C6 glioma cells and increased their migratory capacity [24].

It was suggested that the interaction between tumour and stromal cells can result in altered expression pattern of the tu-
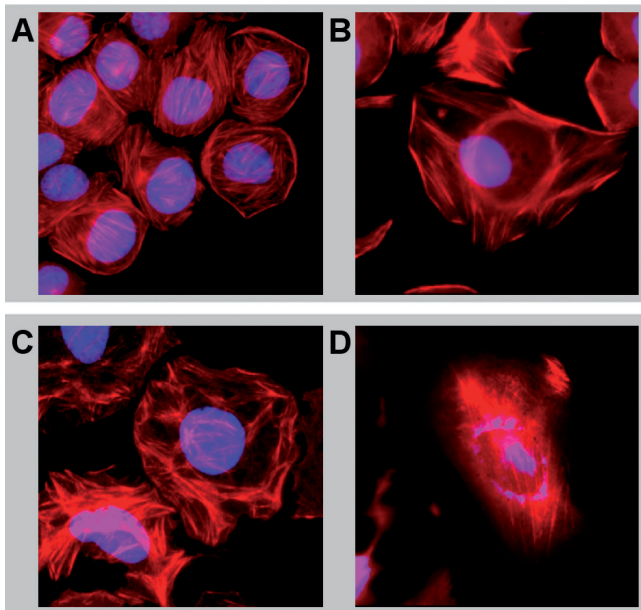
Figure 1. Morphological changes induced by presence of MSC-CM in SK-BR-3 cells (magnification 40x). Cells were cultured in DMEM (A) or MSC-CM (B) for 6 days. Lower density cultures are shown on the left panel and higher density cultures on the right panel. Kinetic-life cell imaging unravelled increased confluence, and shift from epithelial to mesenchymal-like morphology in majority of MSC-CM cultured tumour cells.

mour cells [25-27]. Several mechanisms through which MSCs induce EMT, including the role of MSC's secreted growth factors, cytokines, and chemokines were proposed [28]. Considerably higher gene expression of EMT-associated markers, ranging from 10.7 times for *SNAI1* to more than 2500 times for *SNAI2,* in AT-MSCs in comparison with DMEM cultured SK-BR-3 cells (Figure 4) and their up-regulation after MSC-CM cultivation support this hypothesis.

DNA methylation is not changed during EMT. Alterations in cellular phenotypes, such as EMT, can play a critical role in tumour progression, allowing the tumour cells to acquire "cancer stem-like" properties thus increasing migration and invasion ability and contributing to chemoresistance [29]. The genome-wide loss of DNA methylation accompanied by gene specific hypermethylation is regarded as a common epigenetic event in malignancies and may play crucial roles in carcinogenesis, including regulation of EMT processes and subsequent metastatic spread [30]. Although active acquisition
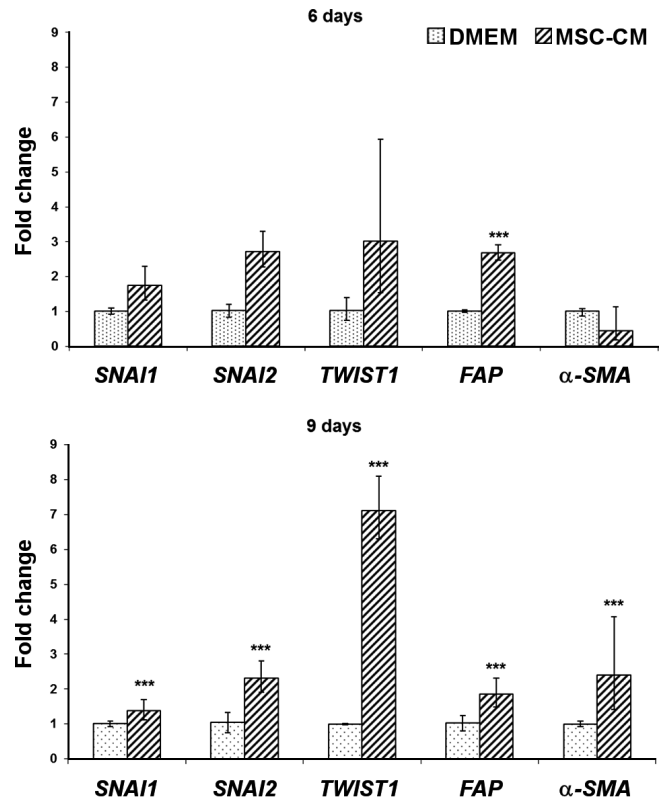
of epigenetic changes is poorly understood, it has been shown recently that sustained induction of EMT activates *de novo* DNA methylation at targeted sites [31]. However, AT-MSC-induced EMT had almost no effect on LINE-1 and gene-specific DNA methylation patterns in our experiments (Figure 5). LINE-1 are highly repeated human retrotransposon sequences and constitute about 17% of the human genome. The CpG sites in a LINE-1 promoter are normally heavily methylated to prevent retrotransposition. Three genes, involved in EMT [15] and presence of CTC in peripheral blood of breast cancer patients [16], were selected for gene-specific DNA methylation analyses. The tissue inhibitors of metalloproteinases (TIMPs) prevent the degradation of the extracellular matrix by these proteases. TIMP3 is a matrix-binding protein that regulates the matrix composition and affects tumour growth, angiogenesis, invasion and metastasis [32]. *BRMS1* is a member of a growing family of metastasis suppressor genes which prevent the development of metastasis without affecting tumour growth
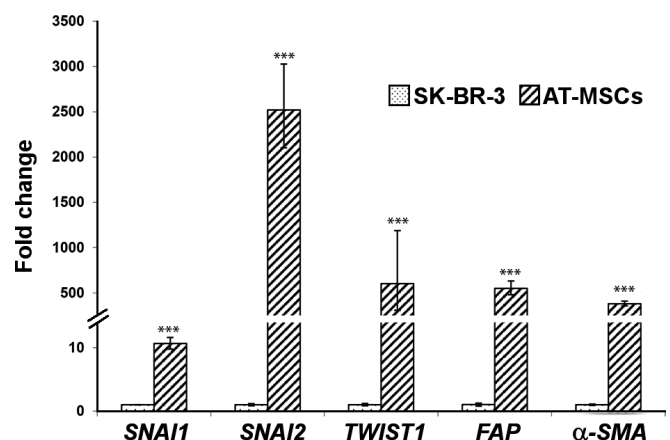
Figure 2. Actin cytoskeleton reorganization resulting from EMT in the presence or absence of AuNPs. DMEM (A) or MSC-CM (B, C, D) cultured SK-BR-3 cells (magnification fluorescent microscopy 630x). After 6 days of cultivation (A, B) cells were treated with 20 nm AuNPs for 24 (C) and 48 hours (D) at concentration 3 μg/ml. Presence of AuNPs caused dynamic changes in actin cytoskeleton highlighted by formation of stress fibers and eventually leading to disruption of F-actin fibers.

Figure 3. Gene expression of EMT-associated markers in SK-BR-3 cells after 6 and 9 days MSC-CM cultivation relative to DMEM only cultured cells. After 6 days significant up-regulation of *FAP* mRNA was detected in MSC-CM cultured cells, while all analysed EMT markers were significantly up-regulated after 9 days of SK-BR-3 cells cultivation in MSC-CM. Error bars represent standard error of the mean normalized expression. *** $P < 0.001$

[33]. The *ADAM23* gene encodes a member of the ADAM (a disintegrin and metalloprotease domain) family. Members of this family are membrane-anchored proteins structurally related to snake venom disintegrins that have been implicated in a variety of biological processes involving cell-cell and cell-matrix interactions [34]. For none of the 3 selected genes altered gene-specific DNA methylation following MSC-CM treatment was detected (Figure 5). Although down-regulation of E-cadherin, coded by *CDH1* gene is considered to be a hallmark of EMT, we did not analyze the DNA methylation level in its promoter, due to the presence of homozygous deletion of exons 2 through 12, reported for the SK-BR-3 cell line [35, 36] and verified by *CDH1* gene expression analysis. Despite the lack of E-cadherin expression, SK-BR-3 cells maintain the epithelial phenotype and easily undergo EMT.

Similarly to our results, a stable pattern of DNA methylation during EMT was reported repeatedly. Liu et al. did not find differentially methylated regions in lung cancer A549 cells treated with TGFβ for 4, 12, 24 or 96 hours [37]. It was shown that while the genome-wide DNA methylation pattern was unchanged during EMT induced by TGFβ in AML12 cells, reprogramming of specific chromatin domains was detected across the genome [38]. Integrated analyses of epigenetic promoter modifications and gene expression changes revealed a strong correlation between histone methylations and gene

Figure 4. Gene expression of EMT-associated markers in AT-MSCs relative to DMEM cultured SK-BR-3 cells. Considerably higher gene expression of EMT-associated markers was detected in AT-MSCs. Error bars represent standard error of the mean normalized expression. *** $P < 0.001$
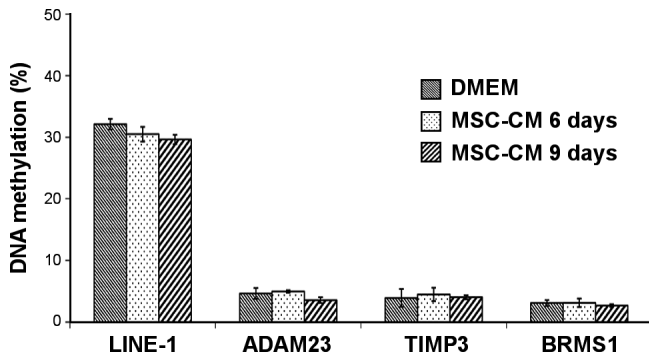
Figure 5. Global and gene specific DNA methylation levels in DMEM and MSC-CM cultivated cells. AT-MSCs induced EMT had almost no effect on LINE-1 and gene specific DNA methylation pattern. DNA methylation levels are presented as mean values; error bars represent standard deviation.
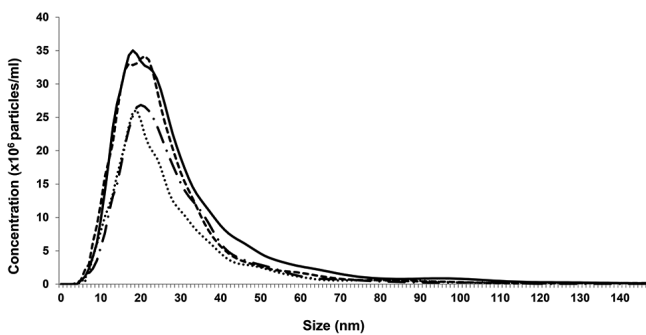

Figure 6. Particle size distribution of 20 nm AuNPs in water used in the *in vitro* experiments (NanoSight NS500). Each line represents one of four independent measurements. Mean measured concentration determined by NTA was $6.98 \times 10^{11} \pm 1.47 \times 10^{11}$ particles per millilitre.
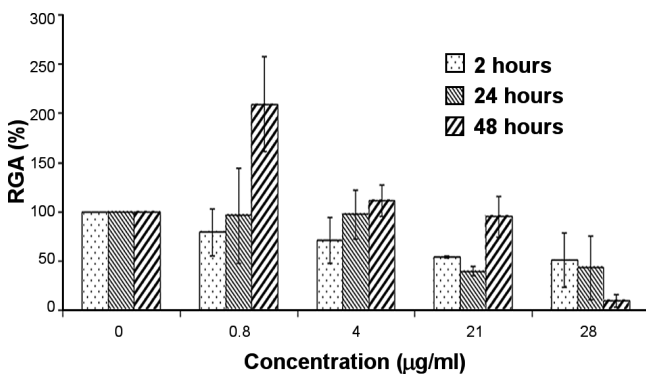

Figure 7. Cytotoxic effects of 20 nm AuNPs on SK-BR-3 cells measured as relative growth activity (RGA). Cells were treated with 4 concentrations (0.8-28 μg/ml) of AuNPs for 2, 24 and 48 hours and cell number was counted immediately after staining. Bars represent growth activity relative to 100% of control. The data are expressed as mean ± SE of the two independent experiments.

expression, while DNA methylation was weakly associated with global gene repression [39].

AuNPs treatment showed moderate EMT inhibitory effect. After induction of EMT by AT-MSCs we analyzed the capability of 20 nm AuNPs to inhibit or reverse EMT in breast cancer cells. Selection of the AuNPs was based on the results of Arvizo *et al.* who, in their experiments aiming to reverse EMT in ovarian cancer cells, tested 5, 20, 50 and 100 nm unmodified AuNPs [11]. They demonstrated that the inhibitory effect is dependent on surface (particle) size, with 20 nm AuNPs showing the greatest efficiency [11]. Prior to beginning *in vitro* experiments, particle size distribution and concentration were determined. The mean size of particles from individual measurements varied from 28 to 38 nm with an average mean size of 33.0 ± 4.08 nm. Mode of peak ranged from 18 to 21 nm with an average modal size 19.5 ± 1.29 nm (Figure 6). The average concentration of particles was $6.98 \times 10^{11} \pm 1.47 \times 10^{11}$ per millilitre which corresponded to the manufacturer's proclaimed value 7×10^{11} particles per millilitre.

The optimal concentration of AuNPs for *in vitro* experiments was established according to the results of RGA (Figure 7). Arvizo et al. demonstrated that the 20 μg/ml concentration of 20 nm unmodified AuNPs was the most effective to inhibit the proliferation of A2780 ovarian cancer cells [11]. Therefore we tested several concentrations of 20 nm AuNPs ranging from 0.8 – 28 μg/ml for 2, 24 or 48 hours. After 48 hours of treatment concentration dependent increase of RGA was observed. Similar findings were published previously for human dermal microvascular endothelial cells (HDMEC) after 48 hour of citrate coated AuNPs treatment [40]. The authors reported significant increase in cell viability compared to the untreated control after the treatment with 500 μM and 1000 μM citrate coated AuNPs. They hypothesised that increase in cell viability may be explained by a higher mitochondrial activity of cells incubated with AuNPs. In addition, a small but not significant increase in cell viability of human cerebral microvascular endothelial cell line (hCMEC) [40] and human alveolar type-II NCIH441 cells were also observed [41].

As the concentrations exceeding 4 μg/ml were cytotoxic (Figure 7), the concentration 3 μg/ml was selected for further experiments aiming to study DNA methylation changes during EMT induction and reversal. AuNPs at concentration 5μg/ml were used by the same group to sensitize ovarian cancer cells to cisplatin. AuNPs prevented cisplatin-induced acquired chemoresistance and stemness in ovarian cancer cells and sensitized them to cisplatin [42].

The morphological changes in SK-BR-3 EMT-induced cells after treatment with 20 nm AuNPs at concentration 3 μg/ml are depicted at Figure 8. EMT-like morphological changes present in EMT-induced cells are clearly less pronounced in AuNPs treated cells and they are more similar to the DMEM control, showing that treatment with AuNPs attenuated the EMT process. These differences were mainly visible after prolonged treatment and are in accordance with that published by Xiong et al. [42]. AuNPs treatment for 24 or 48 hours
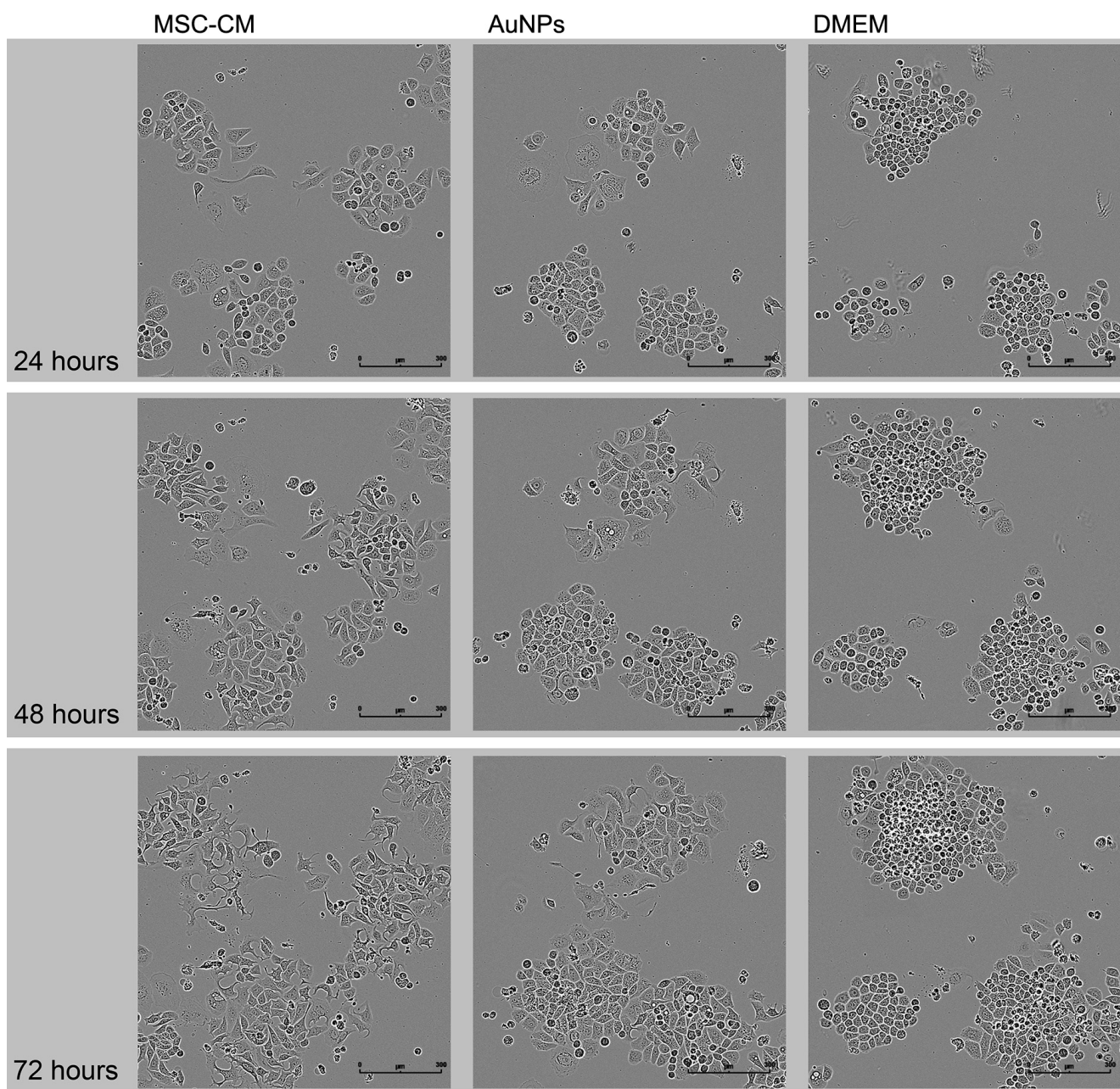
Figure 8. Morphological changes of EMT induced SK-BR-3 cells after treatment with 20 nm AuNPs at concentration 3 μg /ml for 24, 48 and 72 hours in comparison to MSC-CM and DMEM cultured cells (magnification 40x).

induced changes in actin organization eventually leading to disruption of actin fibres (Figures 2C and 2D). After 24 hours of AuNP treatment we found significant down-regulation of gene expression of *SNAI2* (Figure 9). It is difficult to explain significant up-regulation of α-SMA after 48 hours of AuNP treatment. We hypothesise that it could be associated with previously discussed increase in cell viability by AuNPs. Despite the sustained pressure of EMT-inducing factors present in MSC-CM and the lower concentration of AuNPs used in

our experiment in comparison to previously published results [11, 42], our results suggest slight inhibitory effect of AuNPs treatment on EMT in SK-BR-3 cells.

Having in mind the therapeutic potential of nanoparticles, it is critical to understand their ability to affect epigenetic processes in living cells. In our *in vitro* experiments DNA methylation remained relatively stable and was not altered by AuNP treatment (Figure 10). AuNPs have been reported to have excellent biocompatibility [43] and reports of epigenetic
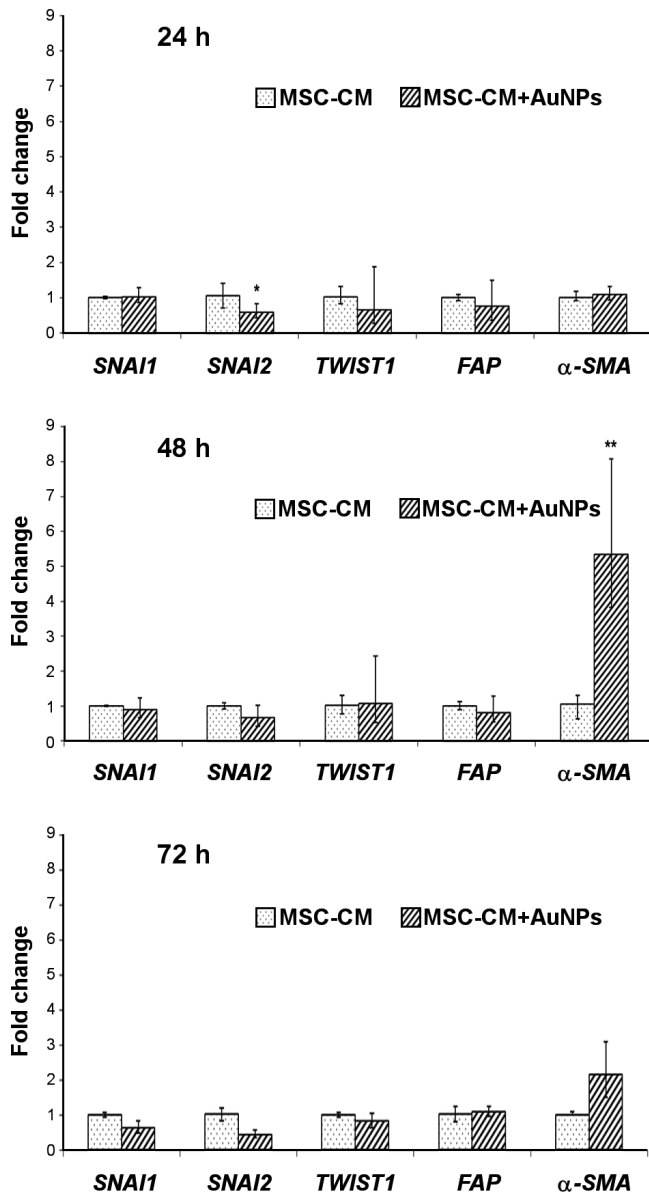
Figure 9. Gene expression of EMT-associated markers in EMT induced SK-BR-3 cells, after treatment with 20 nm AuNPs at concentration 3 μg/ml for 24, 48 and 72 hours, relative to MSC-CM cultivated cells. After 24 hours of AuNP treatment only *SNAI2* gene expression decreased significantly, while significant up-regulation of α-SMA after 48 hours of AuNP treatment was detected. Error bars represent standard error of the mean normalized expression. * P < 0.05, ** P < 0.01
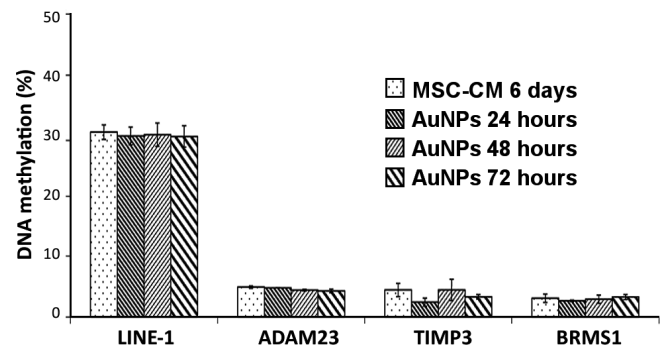

Figure 10. Global and gene specific DNA methylation levels in MSC-CM cultivated and AuNPs treated cells. AuNPs treatment had almost no effect on LINE-1 and gene specific DNA methylation pattern. DNA methylation levels are presented as mean values; error bars represent standard deviation.

able in early phases of EMT but could be rather a marker of the sustained presence of potent EMT-inducing signals. Several lines of evidence have shown that histone modifications precede DNA methylation changes during EMT. The formation of the H3K9me3 mark was demonstrated to be a prelude to the recruitment of DNA methyltransferases that catalyse DNA methylation [47], highlighting the synergistic effect of various epigenetic mechanisms. The regulatory impact of miRNA was reviewed recently, involving the role of epigenetic silencing of cancer-implicated miRNAs by CpG island hypermethylation in human tumour cells [48, 49]. Additional research is needed to provide more comprehensive insights into the dynamics of epigenetic events inducing and accompanying the EMT programme and into the therapeutic potential of AuNPs.

References

[1]   KHAMIS ZI, SAHAB ZJ, SANG QX. Active roles of tumor stroma in breast cancer metastasis. Int J Breast Cancer 2012; 2012: 574025. http://dx.doi.org/10.1155/2012/574025

[2]   MARTIN FT, DWYER RM, KELLY J, KHAN S, MURPHY JM et al. Potential role of mesenchymal stem cells (MSCs) in the breast tumour microenvironment: stimulation of epithelial to mesenchymal transition (EMT). Breast Cancer Res Treat 2010; 124: 317–326. http://dx.doi.org/10.1007/s10549-010-0734-1

effects of AuNPs are rare, and mostly refer to the chromatin or miRNA level [14, 44-46]. The epigenetic safety of AuNPs needs to be further investigated to avoid potential health risks posed by the use of nanomaterials.

The data presented herein demonstrate the ability of AT-MSCs to induce EMT *in vitro* and thus to contribute to breast carcinogenesis. Changes in DNA methylation are not detect-

[3]   ZUK PA, ZHU M, ASHJIAN P, DE UGARTE DA, HUANG JI et al. Human adipose tissue is a source of multipotent stem cells. Mol Biol Cell 2002; 13: 4279–4295. http://dx.doi.org/10.1091/mbc.E02-02-0105

[4]   EL-HAIBI CP, KARNOUB AE. Mesenchymal stem cells in the pathogenesis and therapy of breast cancer. Mammary Gland Biol Neoplasia 2010; 15: 399–409. http://dx.doi.org/10.1007/s10911-010-9196-7

[5]   BHATTACHARYA R, MUKHERJEE P. Biological properties of "naked" metal nanoparticles. Adv Drug Deliv Rev 2008; 60: 1289–1306. http://dx.doi.org/10.1016/j.addr.2008.03.013

[6]   KARNOUB AE, DASH AB, VO AP, SULLIVAN A, BROOKS MW et al. Mesenchymal stem cells within tumour stroma promote breast cancer metastasis. Nature 2007; 449: 557–563. http://dx.doi.org/10.1038/nature06188

[7]   KUCEROVA L, SKOLEKOVA S, MATUSKOVA M, BOHAC M, KOZOVSKA Z. Altered features and increased chemo-sensitivity of human breast cancer cells mediated by adipose tissue-derived mesenchymal stromal cells. BMC Cancer 2013; 13: 535. http://dx.doi.org/10.1186/1471-2407-13-535

[8]   NICKEL A, STADLER SC. Role of epigenetic mechanisms in epithelial-to-mesenchymal transition of breast cancer cells. Transl Res 2015; 165: 126–142. http://dx.doi.org/10.1016/j.trsl.2014.04.001

[9]   LEHMANN U, LANGER F, FEIST H, GLOCKNER S, HASEMEIER B et al. Quantitative assessment of promoter hypermethylation during breast cancer development. Am J Pathol 2002; 160: 605–612. http://dx.doi.org/10.1016/S0002-9440(10)64880-8

[10]   BOISSELIER E, ASTRUC D. Gold nanoparticles in nano-medicine: preparations, imaging, diagnostics, therapies and toxicity. Chem Soc Rev 2009; 38: 1759–1782. http://dx.doi.org/10.1039/b806051g

[11]   ARVIZO RR, SAHA S, WANG E, ROBERTSON JD, BHATTACHARYA R et al. Inhibition of tumor growth and metastasis by a self-therapeutic nanoparticle. Proc Natl Acad Sci U S A 2013; 110: 6700–6705. http://dx.doi.org/10.1073/pnas.1214547110

[12]   ARVIZO RR, RANA S, MIRANDA OR, BHATTACHARYA R, ROTELLO VM et al. Mechanism of anti-angiogenic property of gold nanoparticles: role of nanoparticle size and surface charge. Nanomedicine 2011; 7: 580–587. http://dx.doi.org/10.1016/j.nano.2011.01.011

[13]   SMOLKOVA B, EL YAMANI N, COLLINS AR, GUTLEB AC, DUSINSKA M. Nanoparticles in food. Epigenetic changes induced by nanomaterials and possible impact on health. Food Chem Toxicol 2015; 77: 64–73. http://dx.doi.org/10.1016/j.fct.2014.12.015

[14]   BALANSKY R, LONGOBARDI M, GANCHEV G, ILTCHEVA M, NEDYALKOV N et al. Transplacental clastogenic and epigenetic effects of gold nanoparticles in mice. Mutat Res 2013; 751–752: 42–48. http://dx.doi.org/10.1016/j.mrfmmm.2013.08.006

[15]   JIN H, YU Y, ZHANG T, ZHOU X, ZHOU J et al. Snail is critical for tumor growth and metastasis of ovarian carcinoma. Int J Cancer 2010; 126: 2102–2111. http://dx.doi.org/10.1002/ijc.24901

[16]   CHIMONIDOU M, KALLERGI G, GEORGOULIAS V, WELCH DR, LIANIDOU ES. Breast cancer metastasis suppressor-1 promoter methylation in primary breast tumors and corresponding circulating tumor cells. Mol Cancer Res 2013; 11: 1248–1257. http://dx.doi.org/10.1158/1541-7786.MCR-13-0096

[17]   KUCEROVA L, ALTANEROVA V, MATUSKOVA M, TY-CIAKOVA S, ALTANER C. Adipose tissue-derived human mesenchymal stem cells mediated prodrug cancer gene therapy. Cancer Res 2007; 67: 6304–6313. http://dx.doi.org/10.1158/0008-5472.CAN-06-4024

[18]   PFAFFL MW, HORGAN GW, DEMPFLE L. Relative expression software tool (REST) for group-wise comparison and statistical analysis of relative expression results in real-time PCR. Nucleic Acids Res 2002; 30(9): e36. http://dx.doi.org/10.1093/nar/30.9.e36

[19]   ZMETAKOVA I, DANIHEL L, SMOLKOVA B, MEGO M, KAJABOVA V et al. Evaluation of protein expression and DNA methylation profiles detected by pyrosequencing in invasive breast cancer. Neoplasma 2013; 60: 635–646. http://dx.doi.org/10.4149/neo_2013_082

[20]   KUMAR S, CHANDA D, PONNAZHAGAN S. Therapeutic potential of genetically modified mesenchymal stem cells. Gene Ther 2008; 15: 711–715. http://dx.doi.org/10.1038/gt.2008.35

[21]   LALU MM, MCINTYRE L, PUGLIESE C, FERGUSSON D, WINSTON BW et al. Safety of cell therapy with mesenchymal stromal cells (SafeCell): a systematic review and meta-analysis of clinical trials. PloS One 2012; 7(10): e47559. http://dx.doi.org/10.1371/journal.pone.0047559

[22]   STRIOGA M, VISWANATHAN S, DARINSKAS A, SLABY O, MICHALEK J. Same or not the same? Comparison of adipose tissue-derived versus bone marrow-derived mesenchymal stem and stromal cells. Stem Cells Dev 2012; 21: 2724–2752. http://dx.doi.org/10.1089/scd.2011.0722

[23]   KIM J, ESCALANTE LE, DOLLAR BA, HANSON SE, HE-MATTI P. Comparison of breast and abdominal adipose tissue mesenchymal stromal/stem cells in support of proliferation of breast cancer cells. Cancer Invest 2013; 31: 550–554. http://dx.doi.org/10.3109/07357907.2013.830737

[24]   ISER IC, CESCHINI SM, ONZI GR, BERTONI AP, LENZ, G et al. Conditioned Medium from Adipose-Derived Stem Cells (ADSCs) Promotes Epithelial-to-Mesenchymal-Like Transition (EMT-Like) in Glioma Cells In vitro. Mol Neurobiol 2015; Epub ahead of print. http://dx.doi.org/10.1007/s12035-015-9585-4

[25]   KUCEROVA L, SKOLEKOVA S. Tumor microenvironment and the role of mesenchymal stromal cells. Neoplasma 2013; 60: 1–10. http://dx.doi.org/10.4149/neo_2013_001

[26]   KLOPP AH, GUPTA A, SPAETH E, ANDREEFF M, MARINI F. 3rd. Concise review: Dissecting a discrepancy in the literature: do mesenchymal stem cells support or suppress tumor growth? Stem Cells 2011; 29: 11–19. http://dx.doi.org/10.1002/stem.559

[27]   UNGEFROREN H, SEBENS S, SEIDL D, LEHNERT H, HASS R. Interaction of tumor cells with the microenvironment. Cell Commun Signal 2011; 9: 18. http://dx.doi.org/10.1186/1478-811X-9-18

[28] SCHWEIZER R, TSUJI W, GORANTLA VS, MARRA KG, RUBIN JP et al. The role of adipose-derived stem cells in breast cancer progression and metastasis. Stem Cells Int, 2015; 120949. http://dx.doi.org/10.1155/2015/120949

[29] MANI SA, GUO W, LIAO MJ, EATON EN, AYYANAN A et al. The epithelial-mesenchymal transition generates cells with properties of stem cells. Cell 2008; 133: 704–715. http://dx.doi.org/10.1016/j.cell.2008.03.027

[30] TAM WL, WEINBERG RA. The epigenetics of epithelial-mesenchymal plasticity in cancer. Nat Med 2013; 19: 1438–49. http://dx.doi.org/10.1038/nm.3336

[31] DUMONT N, WILSON MB, CRAWFORD YG, REYNOLDS PA, SIGAROUDINIA M.et al. Sustained induction of epithelial to mesenchymal transition activates DNA methylation of genes silenced in basal-like breast cancers. Proc Natl Acad Sci U S A 2008; 105: 14867–14872. http://dx.doi.org/10.1073/pnas.0807146105

[32] LUI EL, LOO WT, ZHU L, CHEUNG MN, CHOW LW. DNA hypermethylation of TIMP3 gene in invasive breast ductal carcinoma. Biomed Pharmacother 2005; 59: Suppl 2, S363–365. http://dx.doi.org/10.1016/S0753-3322(05)80079-4

[33] METGE BJ, FROST AR, KING JA, DYESS DL, WELCH DR et al. Epigenetic silencing contributes to the loss of BRMS1 expression in breast cancer. Clin Exp Metastasis 2008; 25: 753–763. http://dx.doi.org/10.1007/s10585-008-9187-x

[34] COSTA FF, VERBISCK NV, SALIM AC, IERARDI DF, PIRES LC et al.. Epigenetic silencing of the adhesion molecule ADAM23 is highly frequent in breast tumors. Oncogene 2004; 23: 1481–1488. http://dx.doi.org/10.1038/sj.onc.1207263

[35] Van De Wetering M, Barker N, HARKES IC, VAN DER HEYDEN M, DIJK NJ et al. Mutant E-cadherin breast cancer cells do not display constitutive Wnt signaling. Cancer Res 2001; 61: 278–284.

[36] LOMBAERTS M, VAN WEZEL T, PHILIPPO K, DIERSSEN JWF, ZIMMERMAN RME et al. E-cadherin transcriptional downregulation by promoter methylation but not mutation is related to epithelial-to-mesenchymal transition in breast cancer cell lines. Br J Cancer 2006; 94: 661–671. http://dx.doi.org/10.1038/sj.bjc.6602996

[37] LIU F, ZHOU Y, ZHOU D, KAN M, NIU X et al. Whole DNA methylome profiling in lung cancer cells before and after epithelial-to-mesenchymal transition. Diagn Pathol 2014; 9: 66. http://dx.doi.org/10.1186/1746-1596-9-66

[38] MCDONALD OG, WU H, TIMP W, DOI A, FEINBERG AP. Genome-scale epigenetic reprogramming during epithelial to mesenchymal transition. Nat Struct Mol Biol 2011; 18: 867–874. http://dx.doi.org/10.1038/nsmb.2084

[39] KE XS, QU Y, CHENG Y, LI WC, ROTTER V et al. Global profiling of histone and DNA methylation reveals epigenetic-based regulation of gene expression during epithelial to mesenchymal transition in prostate cells. BMC Genomics 2010; 11: 669. http://dx.doi.org/10.1186/1471-2164-11-669

[40] FREESE C, UBOLDI C, GIBSON MI, UNGER RE, WEKSLER BB et al. Uptake and cytotoxicity of citrate-coated gold nanospheres: Comparative studies on human endothelial and epithelial cells. Part Fibre Toxicol 2012; 9: 1–11. http://dx.doi.org/10.1186/1743-8977-9-23

[41] UBOLDI C, BONACCHI D, LORENZI G, HERMANNS MI, POHL C et al. Gold nanoparticles induce cytotoxicity in the alveolar type-II cell lines A549 and NCIH441. Part Fibre Toxicol 2009; 6: 1–12. http://dx.doi.org/10.1186/1743-8977-6-18

[42] XIONG X, ARVIZO RR, SAHA S, ROBERTSON DJ, MCMEEKIN S et al. Sensitization of ovarian cancer cells to cisplatin by gold nanoparticles. Oncotarget 2014; 5: 6453–6465. http://dx.doi.org/10.18632/oncotarget.2203

[43] SHUKLA R, BANSAL V, CHAUDHARY M, BASU A, BHONDE RR et al. Biocompatibility of gold nanoparticles and their endocytotic fate inside the cellular compartment: a microscopic overview. Langmuir 2005; 21: 10644–10654. http://dx.doi.org/10.1021/la0513712

[44] MAZUMDER A, SHIVASHANKAR GV. Gold-nanoparticle-assisted laser perturbation of chromatin assembly reveals unusual aspects of nuclear architecture within living cells. Biophys J 2007; 93: 2209–2216. http://dx.doi.org/10.1529/biophysj.106.102202

[45] SULE N, SINGH R, SRIVASTAVA DK. Alternative Modes of Binding of Recombinant Human Histone Deacetylase 8 to Colloidal Gold Nanoparticles. Biomed Nanotechnol 2008; 4: 463–468. http://dx.doi.org/10.1166/jbn.2008.011

[46] NG CT, DHEEN ST, YIP WC, ONG CN, BAY BH et al. The induction of epigenetic regulation of PROS1 gene in lung fibroblasts by gold nanoparticles and implications for potential lung injury. Biomaterials 2011; 32: 7609–7615. http://dx.doi.org/10.1016/j.biomaterials.2011.06.038

[47] CEDAR H, BERGMAN Y. Linking DNA methylation and histone modification: patterns and paradigms. Nat Rev Genet 2009; 10: 295–304. http://dx.doi.org/10.1038/nrg2540

[48] ZHANG J, MA L. MicroRNA control of epithelial-mesenchymal transition and metastasis. Cancer Metastasis Rev 2012; 31: 653–662. http://dx.doi.org/10.1007/s10555-012-9368-6

[49] LUJAMBIO A, CALIN GA, VILLANUEVA A, ROPERO S, SANCHEZ-CESPEDES M et al. A microRNA DNA methylation signature for human cancer metastasis. Proc Natl Acad Sci U S A 2008; 105: 13556–13561. http://dx.doi.org/10.1073/pnas.0803055105